The discovery of a forgotten vault in the church of Sainte-Mesme (Essonne)

N. Boubaki, E. Léger, A. Saintenoy
IDES, UMR 8148 CNRS, Université Paris Sud, Orsay, France

***Abstract*—A Ground-Penetrating Radar (GPR) prospection was carried out to sound the ground of the church of Sainte-Mesme, a village close to Dourdan in France. This church was chosen because of the presence of a known underground vault in its south part. We tested the ability of determining the presence of a cavity from amplitude versus offset anomaly observed on multi-offset profile. During the acquisition, the GPR survey gave evidences of another forgotten underground vault in the main choir. Posterior to this discovery an archaeological study was performed in the opened vaults which concluded to the use of both underground rooms in the XIVth century.**

Keywords: Ground-Penetrating radar, cavity, archaeology

I. INTRODUCTION

The detection of underground cavities below buildings is an important topic for archaeologists as well as for safety reasons. Several geophysical non-invasive techniques exist for cavity detection: microgravity [1], electrical resistivity tomography [2], seismics [3] and GPR [4]–[6]. Geophysical surveys inside buildings are not always possible with those methods even if some device adaptation are possible as using a capacitive-coupled resistivity system [7] to make electrical resistivity tomography. To prospect for shallow targets, GPR is easy to use inside buildings as in [4], using shielded antennas, as it is a non destructive method. Possible reflections on side walls exist but they are attenuated by the antenna shielding and do not prevent from detecting targets in the ground.

Knowing the presence of an underground vault in Sainte-Mesme church, we decided to survey its floor to test the GPR alone for cavity detection and the estimation of the cavity dimensions. For the latest, three techniques are tested: multi-offset profiling, migration and hyperbola fitting. Those different methods are applied on simulated radargrams and GPR data acquired on the floor of the church.

II. SITE OF INVESTIGATION AND INSTRUMENTATION

Sainte-Mesme is a small town near Dourdan, a town from the French department Les Yvelines in Ile-de-France. Some archaeologists let us know about an underground vault they knew in the south chapel of the church. In the idea of testing our ability to detect underground cavities inside buildings we conducted a GPR survey using a Mala equipment with a 500 MHz shielded antenna set. We mapped the entire church floor acquiring some mono-offset profiles (Fig. 1) and we acquired two multi-offset profiles (WARR configuration) above the known vault and in the central alley. On the day of the survey we discovered a second vault in the center of the church. We acquired above this area 23 parallel profiles separated by 20 cm to create a pseudo-3D data block.

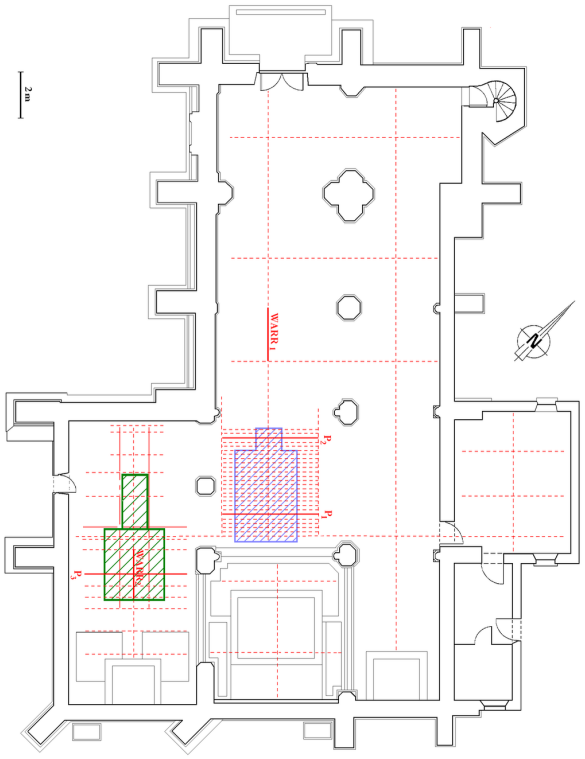

Fig. 1. Plan of the Sainte-Mesme church with localisation of all acquired GPR profiles (red lines), the detailed pseudo-3D acquisition and the underground vaults (in green the known vault, in blue the discovered vault).

III. NUMERICAL SIMULATIONS

Using GprMax2D [8], some simulations are performed to better understand the GPR signal obtained above the vaults.

First we simulate a multi-offset profile supposing a 0.4 m thick layer of electromagnetic velocity 0.13 m/ns (corresponding to a relative dielectric permittivity of 5.32) and an electrical conductivity of 0.02 mS/m, over a 2.4 m thick layer of air. With this model we wish to illustrate an Amplitude

Versus Offset (AVO) effect coming from the Fresnel reflexion coefficients.

The electromagnetic wave will travel through the 0.4 m thick layer, and will arrive to the boundary between the bulk material and the air, with an incident angle θ_i. According to the Snell-Descartes law one part of the energy will be transmitted down to the air, the other part being reflected back. The continuity of Maxwell equations on boundaries give us relations between transmitted and reflected fields [9]. Working in electrical transverse mode (antennas are parallel to the ground, thus to the boundaries), we obtain the following expression for the reflection coefficient R, being the ratio between reflected and original incoming field,

$$R = \frac{\sqrt{\varepsilon_1}\cos(\theta_i) - \sqrt{\varepsilon_2}\sqrt{1 - \frac{\varepsilon_1}{\varepsilon_2}\sin^2(\theta_i)}}{\sqrt{\varepsilon_1}\cos(\theta_i) + \sqrt{\varepsilon_2}\sqrt{1 - \frac{\varepsilon_1}{\varepsilon_2}\sin^2(\theta_i)}} , \qquad (1)$$

with θ_i the incident angle, ε_1 the dielectric permittivity of the first media (in our case $\varepsilon_1 = 5.32$), and ε_2 the dielectric permittivity of the second media (in our case, $\varepsilon_2 = 1$). In our example, $\varepsilon_2 < \varepsilon_1$ induces a critical angle $\theta_c = \sin^{-1}\left(\sqrt{\frac{\varepsilon_1}{\varepsilon_2}}\right)$ from which all the incident energy will be reflected. For incident angles greater than θ_c the reflexion coefficient R becomes complex (Eq. 1). Whereas its amplitude will be equal to unity, its real part is expressed as

$$Real(R) \;=\; \frac{\varepsilon_1\cos(2\theta_i) + \varepsilon_2}{\varepsilon_1 - \varepsilon_2} . \qquad (2)$$

In the WARR configuration, the offset can be computed by geometrical relation, $X = 2d\tan\theta_i$, where d is the thickness of the top layer. Figure 2 shows the real part of the reflection coefficient as a function of the offset. Related to the complex form of the reflected coefficient, the wave will undergo a phase shift, due to the refraction of the incoming waves. This phase shift is of 90° when the real part of the reflection coefficient is 0, obtained for the particular offset $X_p = 2d\tan(\cos^{-1}(\frac{\varepsilon_2}{2\varepsilon_1}))$. With our numerical value, $X_p = 0.97$ m. The phase shift is visible on the reflection underlined in red in Fig. 3.

As a second set of simulations, we computed one radargram acquired above a 2D model designed to represent the vault shape (Fig. 4). The surrounding medium is assigned a relative permittivity of 5.32 and the electrical conductivity is set to 0.02 mS/m. We tested two data processing techniques for determining the size of the vault on this simulated radargram, supposing we know the electromagnetic wave velocity from a multi-offset profile: i) migration was uneasy because of the 2D distribution of the velocity. The reflection on the vault floor is not correctly migrated. One multiple reflection of the roof of the cavity is clearly visible inside after the primary reflection; ii) assuming the first reflection coming from a cylindrical object inside a medium of velocity 0.13 m/ns, hyperbola adaptation using REFLEXW [10] gives an estimate of the radius of the object to be 1.5 m. This technique seems more promising but it relies on the accurate estimation of the top layer velocity.

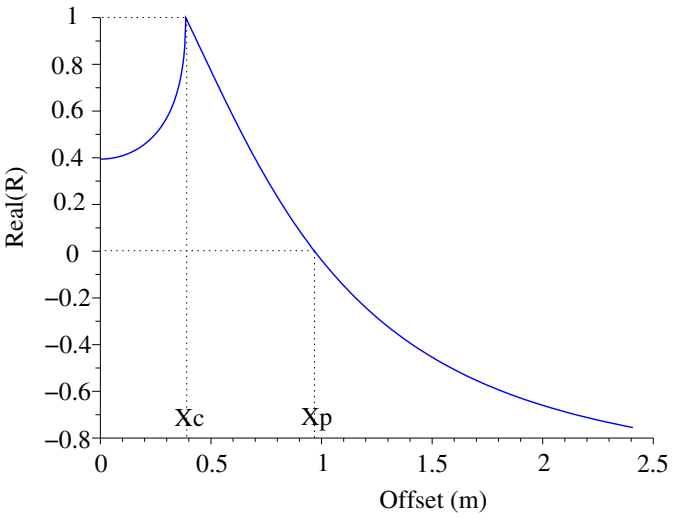

Fig. 2. Real part of the reflection coefficient, with the offset X, related to the incident angle θ_i. X_c corresponds to the offset at the critical angle θ_c, and X_p corresponds to the offset for which $Real(R) = 0$.

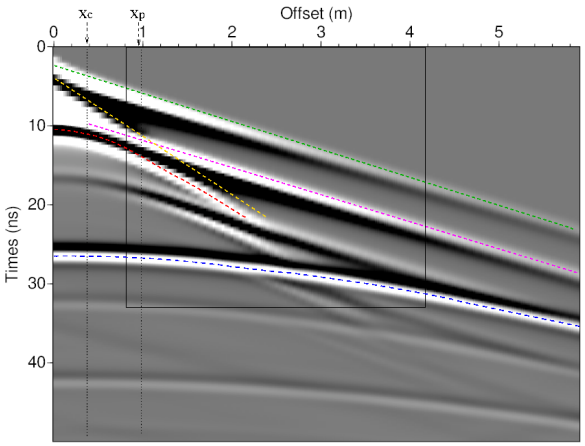

Fig. 3. Simulation of one multi-offset profile. The maxima of the wavelet related to the direct air wave is underlined in green. Those related to the direct ground wave, in yellow, the refracted wave after the critical offset X_c, in pink, the reflection on the roof of the cavity is in red and the reflection on its floor is in blue. The wave reflected on the roof, in red, is subject to some phase shift especially noticeable around the distance X_p. The black box indicates the position of the data shown in Fig. 8.

From those simulations, we conclude that in prospecting for cavities below the ground with GPR, we should i) survey the floor using a mono-offset configuration, looking for areas presenting strong reflections in the radargrams, ii) acquire multi-offset profiles above those anomalous zone (when they are large enough to do so). In theory, we should observe in a multi-offset profile acquired above a cavity a phase reversal of the reflection on the cavity roof.

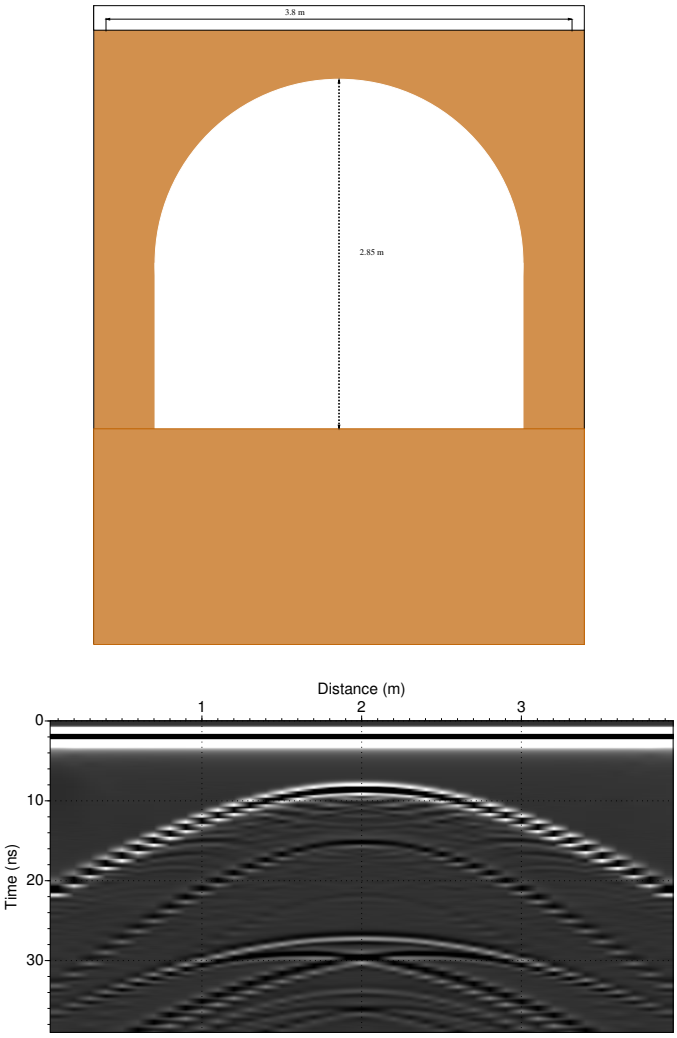

Fig. 4. Model (top) used to numerically simulate the radargram (bottom) over an empty vault.

IV. GPR SURVEY RESULTS

The mono-offset profile in Fig. 5 was acquired across the discovered northern crypt body (see Fig. 1 for profile localisation). The comparison between the simulated radargram (Fig. 4) and the acquired one (Fig. 5) gives a clear interpretation of the acquired profile. The reflection on the floor-air interface is clearly visible. A light reflection (almost as a shadow) appears 4 ns above this one. It can be interpreted as the reflection on the masonry of the crypt.

Fig. 6 shows a mono-offset profiles acquired across the entrance of the northern crypt. The pseudo 3D data block of Fig. 7 helped us to understand the crypt configuration with its entrance position, reported as the blue area on Fig. 1.

The multi-offset profile acquired above the South vault is shown in Fig. 8. Unfortunately, using shielded antenna the smallest offset we could get is 0.8 m. With this smallest offset it is quite difficult to interpret the first reflection and its eventual phase shift. However, comparing with the simulated

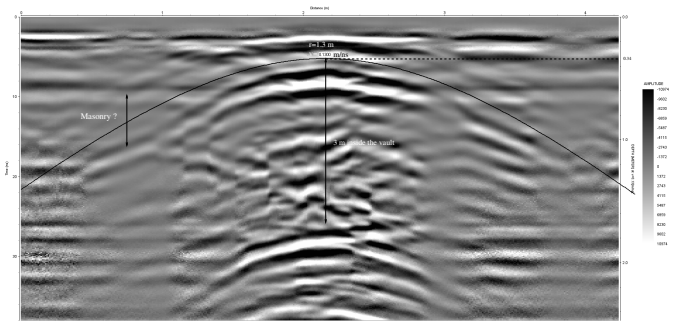

Fig. 5. Radargram acquired across the North vault (P1) using .

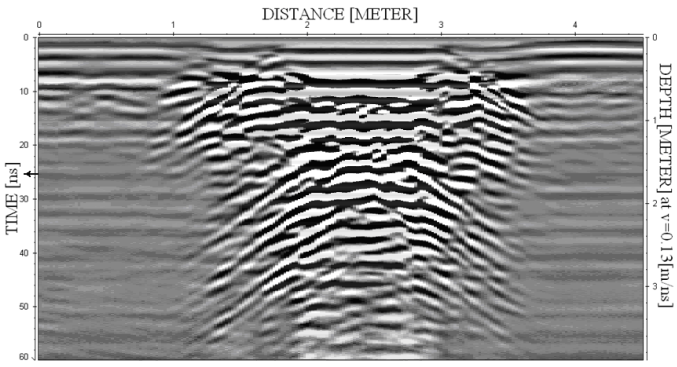

Fig. 6. Radargram acquired across the entrance of the North vault (P2).

radargram of Fig 3, we estimated the electromagnetic velocity of the top layer to be 0.13 m/ns. Supposing this velocity, the reflection on the top of the vault observed in Fig. 5 is fitted by an hyperbola coming from a 1.3 +/- 0.2 m radius cylinder. This hyperbola fits well the right part of the crypt roof but not its left part, where its geometry seems to be different than a cylinder. The top layer is 0.34 m thick and the vault height is estimated to 3 m.

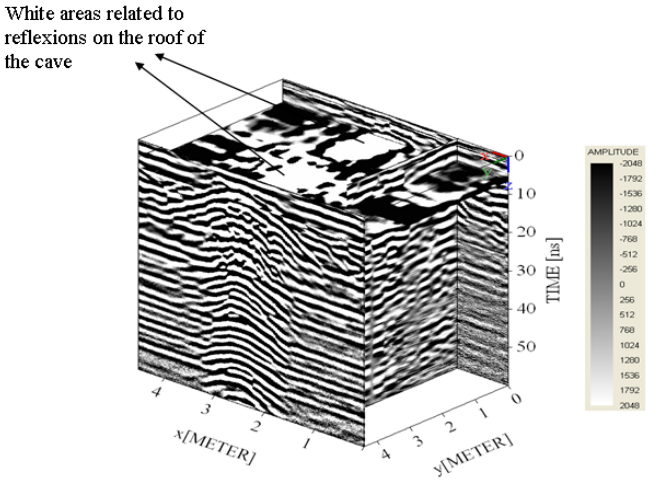

Fig. 7. 3D view of all the radargrams.

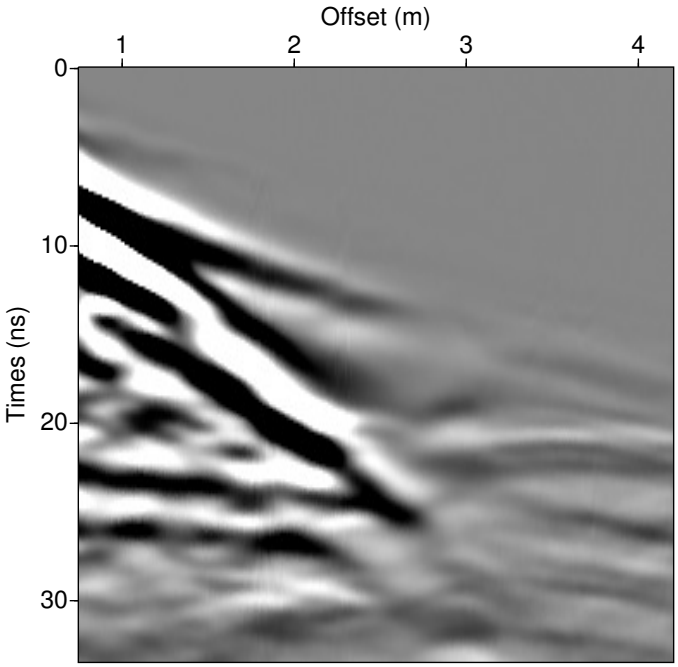

Fig. 8. Multi-offset profile acquired on the floor of the church above the South vault (referred as WARR2 in Fig 1).

V. CONCLUSIONS

We numerically investigated an amplitude versus offset phenomenon when doing some GPR bistatic acquisition above a cavity embedded in an homogeneous ground. We showed results from a GPR survey conducted in the church of Sainte-Mesme. Whereas the AVO is not easy to see in our real data (we will repeat those measurements with smallest offset), this survey gave evidences for the presence of a vault in the center part of the church. The size of the vault has been estimated from GPR analysis using hyperbola adaptation technique to be under a 0.34 m thick layer, including the crypt masonry, with an inside height of 3 m and width of 2.6 +/- 0.4 m. The entrance of the vault was indicated on the radargrams. One year after following its discovery, the vault has been opened and an archaeological study was done [11]. Its width was measured to 2.8 m and its maximum height to 3 m (see Fig. 9). The archaeological study concluded on some different uses of the vaults, the oldest one being for corpse disposal in the XIVth century.

ACKNOWLEDGMENT

We warmly thank Mr Giganon for introducing us to Louis Dejean, president of the association AHASM, as well as Dr Charlier to letting us know about the results of his archaeological study.

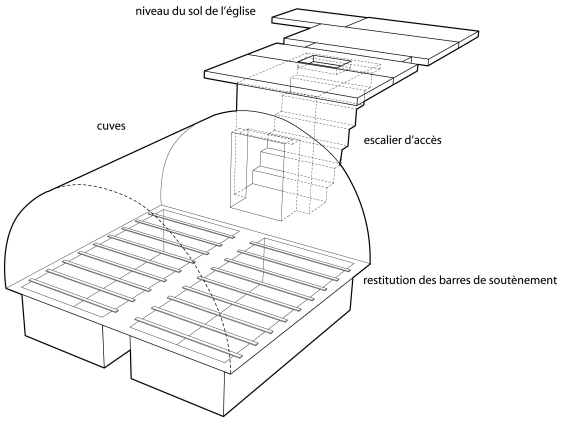

Fig. 9. Schema of the discovered vault (from Charlier et al., 2009).

REFERENCES

[1] D. Patterson, J. C. Davey, A. H. Cooper, and J. K. Ferris, "The application of microgravity geophysics in a phased investigation of dissolution subsidence at Ripon, Yorkshire," *Quarterly Journal of Engineering Geology*, vol. 28, pp. 83–94, 1995.

[2] L. Orlando, "GPR to constrain ERT data inversion in cavity searching: theoretical and practical applications in archaeology," *Journal of Applied Geophysics*, vol. 89, pp. 35–47, 2013.

[3] G. Grandjean and D. Leparoux, "The potential of seismic methods for detecting cavities and buried objects: experimentation at a test site," *Journal of Applied Geophysics*, vol. 56, no. 2, pp. 93–106, 2004.

[4] D. Barilaro, C. Branca, S. Gresta, S. Imposa, A. Leone, and D. Majolino, "Ground Penetrating Radar (G.P.R.) surveys applied to the research of crypts in San Sebastiano's church in Catania (Sicily)," *Journal of Cultural Heritage*, vol. 8, pp. 73–76, 2007.

[5] N. Boubaki, A. Saintenoy, and P. Tucholka, "GPR profiling and electrical resistivity tomography for buried cavity detection: A test site at the abbaye de l'Ouye (France)," in *Advanced Ground Penetrating Radar (IWAGPR), 2011 6th International Workshop on*, 2011, pp. 1–5.

[6] N. Boubaki, A. Saintenoy, S. Kowlaczyk, R. Mieszkowski, F. Welc, J. Budziszewski, and P. Tucholka, "Ground-penetrating radar prospection over a gallery network resulting from neolithic flint mine (Borownia, Poland)," in *Ground Penetrating Radar (GPR), 2012 14th International Conference on*, 2012, pp. 610–615.

[7] C. Neukum, C. Grtzner, R. Azzam, and K. Reicherter, "Mapping buried karst features with capacitive-coupled resistivity system (CCR) and Ground Penetrating Radar (GPR)," in *Advances in Research in Karst Media*, ser. Environmental Earth Sciences, B. Andreo, F. Carrasco, J. J. Durn, and J. W. LaMoreaux, Eds. Springer Berlin Heidelberg, 2010, pp. 429–434.

[8] A. Giannopoulos, "Modelling Ground Penetrating Radar by GprMax," *Construction and building materials*, vol. 19, no. 10, pp. 755–762, 2005.

[9] M. Born and E. Wolf, *Principles of optics: electromagnetic theory of propagation, interference and diffraction of light*, 7th ed. Cambridge University Press, 1999.

[10] K. J. Sandmeier, *Reflexw manual, version 4.5*, www.sandmeier-geo.de, July 2007.

[11] P. Charlier, Y. Ubelmann, I. Huynh-Charlier, J. Gonin, J. Poupon, and L. Brun, "Les pourrissoirs médiévaux de l'église paroissiale de Sainte-Mesme (Yvelines)," in *2e colloque international de pathographie*, D. Boccard, Ed., 2009.